Food Chemistry: X 22 (2024) 101389

Contents lists available at ScienceDirect

Food Chemistry: X

journal homepage: www.sciencedirect.com/journal/food-chemistry-x

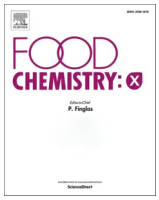

Effects of plasma-activated slightly acidic electrolyzed water on salmon myofibrillar protein: Insights from structure and molecular docking

Guizhi Tan [a,1], Yue Ning [a,1], Chaonan Sun [a], Ying Bu [a], Xiaomin Zhang [b], Wenhui Zhu [a,*], Jianrong Li [a], Xuepeng Li [a,*]

[a] College of Food Science and Engineering, Bohai University, National & Local Joint Engineering Research Center of Storage, Processing and Safety Control Technology for Fresh Agricultural and Aquatic Products, Jinzhou, Liaoning 121013, China
[b] Jinzhou experimental school, Jinzhou, Liaoning 121013, China

ARTICLE INFO

Keywords:
Low-temperature plasma
Slightly acidic electrolytic water
Myofibrillar protein
Protein conformation
Molecular docking

ABSTRACT

The present study investigated the impact of plasma-activated water (PAW), slightly acidic electrolytic water (SAEW) and plasma-activated slightly acidic electrolytic water (PASW) treatment on myofibrillar protein (MP) in salmon fillets. Additionally, the interaction mechanism between myosin and reactive oxygen species was explored by molecular docking. Compared with the control group (719.26 nm), PASW treatment group exhibited the smallest particle size (408.97 nm). The PASW treatment exhibited efficacy in reducing MP aggregation and inhibiting protein oxidation. In comparison with other treatments, PASW treatment demonstrated a greater ability to mitigate damage to the secondary and tertiary structures of MP. O_3 and H_2O_2 interact with myosin through hydrogen bonding. Specifically, O_3 interacts with Lys676, Gly677, and Met678 of myosin while H_2O_2 binds to Thr681, Asp626, Arg680, and Met678. This study offers novel insights into the impact of PASW on MP, and provides a theoretical foundation for its application in aquatic product processing.

1. Introduction

Over the past decades, high temperature and pasteurization have emerged as the primary methods for sterilizing and preserving food. The processing methods, while effective in extending the shelf life of foods, can induce alterations in texture, aroma, and color. Additionally, protein denaturation and oxidation may occur due to excessive heat exposure (Pankaj, Wan, & Keener, 2018). To overcome these limitations, emerging non-thermal food processing technologies have been promoted as viable alternatives to traditional methods, including pulsed light, high-intensity ultrasound, ionizing radiation, hydrostatic pressure, ultraviolet light, slightly acidic electrolyzed water (SAEW) and cold plasma (CP), all of which have demonstrated significant potential in effectively eliminating spoilage and pathogenic microorganisms from food products while preserving their quality characteristics and nutritional value (Olatunde & Benjakul, 2018).

The emerging non-thermal processing technologies, SAEW and CP, have gained significant attention from the scientific community in recent years. CP undergoes various physical and chemical reactions during gas ionization, resulting in the formation of numerous new substances such as reactive oxygen (ROS, such as O_3, H_2O_2, O_2^-), reactive nitrogen (RNS, such as NO_2^-, NO_3^-), free radicals (OH·), and ultraviolet light emissions (Feizollahi, Misra, & Roopesh, 2021). Due to the antimicrobial properties of these substances, CP has been widely utilized for microbial decontamination and preservation of fresh products such as fish, shrimp and meat (Li et al., 2023). The plasma jet device was capable of generating plasma-activated water (PAW), which contains abundant active substances that can effectively disrupt cell membranes and damage intracellular macromolecules such as nucleic acids and proteins, thereby exhibiting excellent sterilization properties (Ma, Zhang, Lv, & Sun, 2020). However, the presence of free radicals in CP may result in alterations to food composition and induce protein oxidation (Perez-Andres, Charoux, Cullen, & Tiwari, 2018). Nyaisaba et al. (2019) found that dielectric blocking discharge (DBD) plasma treatment could enhance the gel properties of squid gels, but it also leads to protein oxidation. The main active ingredient produced by SAEW is hypochlorous acid (HOCl), an efficient germicidal compound that is 80 times more effective than an equivalent concentration of hypochlorite

* Corresponding authors.
E-mail addresses: wenhuiby130@163.com (W. Zhu), xuepengli8234@163.com (X. Li).
[1] Guizhi Tan and Yue Ning should be considered joint first author.

https://doi.org/10.1016/j.fochx.2024.101389
Received 21 December 2023; Received in revised form 27 March 2024; Accepted 11 April 2024
Available online 13 April 2024

ion (ClO^-) (Cao, Zhu, Shi, Wang, & Li, 2009). SAEW has been recognized as an effective bactericidal agent with free chlorine, while elevated concentrations of SAEW have been found to stimulate protein oxidation (Cichoski et al., 2019). In order to address the drawback of protein and lipid oxidation associated with these two sterilization methods, we previously investigated a novel technology known as low temperature plasma activated slightly acidic electrolysis (PASW), which effectively enhances the quality of salmon (Zhu et al., 2023). However, their impact on aquatic proteins remains insufficiently explored, and the intricate interplay between protein and PASW warrants further investigation.

Therefore, this study aimed to investigate the effect of PAW, SAEW and PASW on physicochemical properties, oxidization and structure of myofibrillar protein (MP) in salmon. Moreover, molecular docking was conducted to reveal the interaction between myosin and ROS (O_3, H_2O_2), providing a theoretical framework for elucidating the impact of PASW on aquatic protein at the molecular level.

2. Material and methods

2.1. Material

Atlantic salmon fillets weighing approximately 500 g were procured from Shandong Meijia Group Co. Ltd. (Shandong, China) and stored at −80 °C before use. All chemicals utilized in the present study were of analytical grade and sourced from Sinopharm Chemical Reagent Co., Ltd. (Shanghai, China).

2.2. Salmon fillets treatments

2.2.1. PAW treatment

The PAW solution was produced by subjecting 400 mL of distilled water to atmospheric pressure plasma jet (APPJ, Dongxin High-tech Automation Equipment Co., Ltd., Shenzhen, China) treatment in an ice bath at 320 W for 5 min. The salmon fillets weighing 20 g were completely immersed in a sterile polyethylene bag (Bkmam Biotechnology Co., Ltd., Changde, China) with a thickness of approximately 0.085 mm, containing PAW solution with a mass ratio of 1:6 at room temperature for a duration of 20 min. Subsequently, the treated salmon fillets were utilized for MP extraction.

2.2.2. SAEW treatment

The SAEW was generated using an oxidizing redox potential water generator (DCW, Nordborg, Denmark), resulting in a pH of 6.09, oxidizing redox potential (ORP) of 810 mV, and available chlorine concentration (ACC) of 50 mg/L. The salmon fillets weighing 20 g were completely immersed in a sterile polyethylene bag, containing SAEW solution with a mass ratio of 1:6 at room temperature for 20 min. Subsequently, the treated salmon fillets were utilized for MP extraction.

2.2.3. PASW treatment

PASW was generated by treating SAEW (400 mL) in an ice bath with APPJ at 320 W for 5 min. The salmon fillets weighing 20 g were completely immersed in a sterile polyethylene bag, containing PASW solution with a mass ratio of 1:6 at room temperature for 20 min. Subsequently, the treated salmon fillets were utilized for MP extraction.

2.3. MP extraction

The preparation of MP was conducted in accordance with the method outlined by Zhu et al. (2022) with minor adaptations. 20 g of minced salmon was added to 4 times the volume of 20 mmol/L Tris-HCl (pH 7.2), the mixture was homogenized 30 s at 6000 r/min, followed by centrifugation at 6000 ×*g* for 15 min at 4 °C. Repeated the above steps twice. Subsequently, the precipitate obtained in the last step was mixed with 4 times the volume of extraction buffer (20 mmol/L Tris-HCl, 0.6 mol/L NaCl, pH 7.2), homogenized and centrifuged. The ultimate resolution was deemed to be MP.

2.4. Protein denaturation

2.4.1. Solubility, particle size and turbidity

The solubility and turbidity were measured using the method following Zhu et al. (2022) with some modifications. The MP samples were centrifuged with an Allegra TM 64R (Beckman, Germany) centrifuge at 10000 ×*g* for 15 min at 4 °C, and the resulting supernatant was collected. Solubility was determined as the ratio of protein concentration in the supernatant to that in the original sample before centrifugation. The protein solution was diluted to a 1 mg/mL and subjected to a reaction at 25 °C for 20 min. The particle size distribution of MP solutions was determined using a Nano-ZS90 particle size analyzer (Malvern Instruments Co. Ltd., Worcestershire, UK) at 25 °C. Turbidity was quantified by recording the absorbance at 340 nm with an UV–vis spectrophotometer (UV5, Mettler Toledo, Switzerland).

2.4.2. Surface hydrophobicity

The surface hydrophobicity of MP was evaluated using the method described by Cheng, Zhu, and Liu (2020). The content of surface hydrophobicity was determined by measuring Bromophenol blue bound (BPB bound) (μg) and calculated using the following equation:

$$\text{BPB bound}\ (\mu g) = 100\ \mu g \times \left(OD_{Control} - OD_{Sample}\right) / \left(OD_{Control}\right)$$

2.5. Protein oxidation

2.5.1. Total sulfhydryl and carbonyl contents

Total sulfhydryl content was quantified using the 5,5-dithio-bis (2-nitrobenzoic acid) (DTNB) method, while carbonyl content was estimated through incubation with 2,4-dini-trophenylhydrazine (DNPH), following the protocol of He et al. (2018).

2.5.2. Dityrosine content

The MP was diluted to a concentration of 1.0 mg/mL, followed by filtration and determination of the protein concentration using the biuret method. Subsequently, dityrosine content was quantified via a 970CRT fluorescence spectrophotometry (Shanghai Precision Scientific Instrument Co., Ltd., Shanghai, China). The excitation wavelength was set at 325 nm, and the scanning range covered from 300 to 500 nm with a slit width of 2.5 nm for both excitation and emission light. The fluorescence value was corrected by normalizing to the protein concentration (mg/mL) and expressed in arbitrary units (A.U.) (Davies, Delsignore, & Lin, 1987).

2.6. Protein conformation analysis

2.6.1. Intrinsic fluorescence spectrum

The protein solution was diluted to a concentration of 0.1 mg/mL using 50 mmol/L phosphate buffer (pH 7.0). The intrinsic fluorescence spectra were measured utilizing a fluorescence spectrophotometer with the following parameters: excitation wavelength of 295 nm, slit widths of EX slit 2.5 nm and EM slit 5 nm, and scanning range from 320 to 460 nm (Zhu et al., 2022).

2.6.2. Synchronous fluorescence spectroscopy

Synchronous fluorescence spectrometry was performed with slight modifications to the method described by Shen, Zhao, and Sun (2019). The protein solution was diluted to a concentration of 1.0 mg/mL and measured using a fluorescence spectrophotometer with excitation wavelengths ranging from 200 to 350 nm, Δλ set at both 15 nm and 60 nm, slit width of 2.5 nm, and transmitting slit width of 2.5 nm.

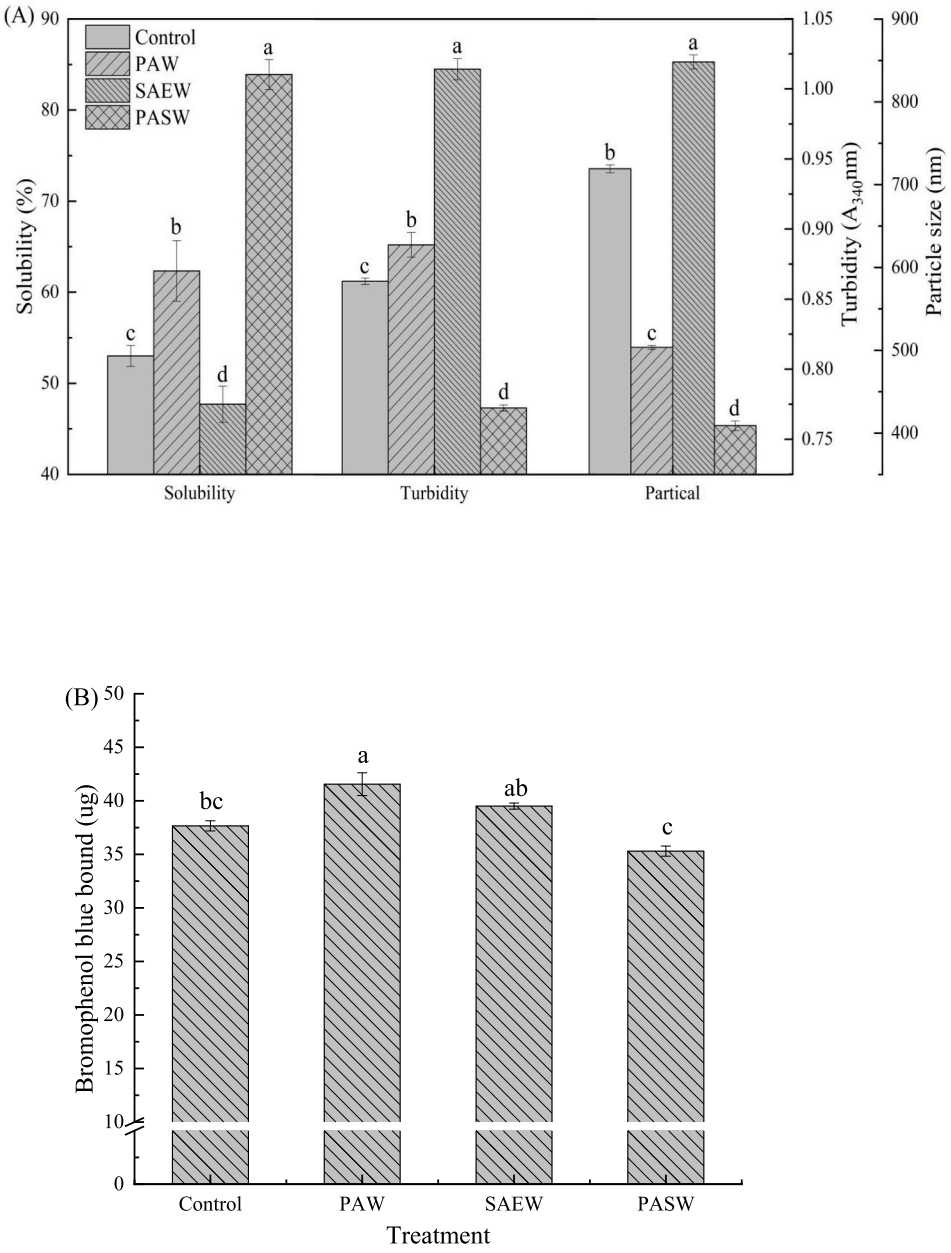

Fig. 1. Effects of different sterilizing methods on solubility, particle size, turbidity (A) and surface hydrophobic (B) of myofibrillar protein. Control, fresh salmon; PAW, plasma activation of water; SAEW, slightly acidic electrolytic water; PASW, low-temperature plasma assisted slightly acidic electrolytic water. Different letters (a-d) show statistically significant difference ($P < 0.05$).

2.6.3. UV absorption spectrum

The UV absorption spectrum of the sample solution (1.0 mg/mL) was measured using the UV adsorption spectra, with a measurement wavelength range set between 220 and 360 nm (Zhu et al., 2022).

2.6.4. Raman spectroscopy

Raman spectroscopy was performed according to the method described by Pan, Guo, Li, Song, and Ren (2017) using a high resolution Raman Spectrometer (Labram HR Evolation, Horiba Jobin Yvon SAS, Longjumeau, France) with an excitation wavelength of 532 nm. The MP samples were mounted onto microscope slides and subjected to signal acquisition for 30 s, with two scans and a Raman shift range of 400–3600 cm^{-1}. The Peak Fit 4 software was utilized for deconvolution to obtain the peak intensity, followed by calculation of the percentages of α-helix, β-fold, β-angle and irregular curling structures.

2.7. Laser scanning confocal microscopy (LSCM)

The protein microstructure changes were directly observed using LSCM, following the method described by Qian et al. (2021) with slight modifications. The MP solution (1 mL) was diluted to a concentration of 2 mg/mL under light-protected conditions. A drop of 10 μL staining solution was placed on a slide and covered with a coverslip. The size and distribution of proteins were visualized at an excitation wavelength of 633 nm using a STELLARIS laser scanning confocal microscopy (Leica, Germany).

2.8. Homology modeling of salmon myosin

The complex structure of salmon myosin necessitated the use of multi-template modeling in SWISS-MODEL (https://swissmodel.expasy.org/interactive) to construct the crystal structure of salmon myosin. The

salmon myosin heavy chain sequence was obtained from the NCBI database (https://www.ncbi.nlm.nih.gov/). Its numbering was XP_014030282.1. The obtained protein sequences were searched for templates by SWISS-MODEL, included F1R3G4, 6XE9, 4PD3, 3DTP, 3JAX, 6Z47, 5I4E, 5JLH, 7MF3, 1JWY, 2AKA, 1MVW, 2W4A, 1G8X, 2W4H, 2W4G, 3MNQ, 1W9L, 1W9K, 4Z1M, 6ZQN, 1EFR, 6J5K, 6J5J, and 6YNY. After aligning the selected templates and aligning them to the myosin heavy chain sequence, models were constructed. According to the global quality estimation score (GMQE) and identity scores, the final model was selected. The model was evaluated by SAVES6 and Ramachandran plot (https://saves.mbi.ucla.edu/) programs.

2.9. Molecular docking

The three-dimensional structure of ozone (O_3) and hydrogen peroxide (H_2O_2) were constructed by Discovery Studio (DS) 2017. The structures were optimized and added CHARMM force field with Minimization ligand protocol (Liu, Bu, Zhu, Li, & Li, 2023). The salmon myosin was treated by Prepare Protein protocol. Salmon myosin was employed as the receptor structure, while ozone and hydrogen peroxide served as ligands. The semi-flexible molecular docking of salmon myosin and O_3/H_2O_2 were compiled through the CDOCKER protocol. Set the Pose Cluster Radius as 0.5. The docking results with the lowest energy were selected for analysis post-docking. The docked cavity coordinates (X = −15.7, Y = 26.7, Z = 141.8) were automatically predicted and chosen using Discovery Studio.

2.10. Statistical analysis

The data were obtained through three independent experiments, and the results are reported as mean ± standard deviation. The experimental data were analyzed by one-way ANOVA using SPSS 19.0 (SPSS Inc., Chicago, IL, USA). The calculated means were compared for significant differences ($P < 0.05$) by Duncan multiple range procedure. Figures were constructed via Origin Pro 9.0 (OriginLab Co., Northampton, USA).

3. Results and discussion

3.1. Protein denaturation

3.1.1. Solubility, particle size and turbidity

Protein solubility is a crucial indicator of meat quality due to its strong correlation with various other functional properties (Sharafodin & Soltanizadeh, 2022). The variations in the solubility of MP in salmon fillets subjected to different sterilization methods were illustrated in Fig. 1A. Compared to the control group, PASW treatment group (83.90%) increased the solubility of MP over other treatments ($P < 0.05$), followed by PAW treatment group (62.33%). This may be attributed to ·OH radicals generated during low temperature plasma treatment, which partially extend protein molecules by breaking non-covalent bonds and electrostatic interactions, thereby enhancing the interaction between protein molecules and water (Zhao & Yang, 2012). The solubility of salmon MP treated with SAEW was reduced, likely due to the unfolding of the protein's spatial structure induced by active substances (ClO^-) in SAEW. This exposure of previously buried hydrophobic groups within the protein molecule and subsequent interaction between them may lead to aggregation, coagulation, and precipitation, ultimately resulting in decreased protein solubility (Ekezie, Cheng, & Sun, 2019). Zhang et al. (2021) discovered that the treatment of soybean isolate protein with CP resulted in an increase in solubility compared to untreated proteins, and this finding is consistent with our research.

The extent of protein denaturation can be quantified by indicators such as solubility, turbidity, and particle size. A decrease in solubility corresponds to an increase in turbidity and particle size, indicating a more severe protein denaturation (Amiri et al., 2021; Ekezie et al., 2019). Different sterilization methods had a significant impact on the particle size of salmon MP. The untreated salmon MP exhibited a particle size of 719.26 nm, whereas PAW-treated, SAEW-treated and PASW-treated salmon displayed respective particle sizes of 503.44 nm, 848.24 nm and 408.97 nm. Sun, Dai, Liu, and Gao (2016) demonstrated that reducing the particle size of proteins can effectively enhance their physical and chemical properties. SAEW caused a significant increase in particle size, possibly due to oxidative modification of the protein disrupting the equilibrium between protein molecules and their interactions with water, thus leading to cross-linked polymerization and formation of large protein aggregates. Li et al. (2020) subjected zein alcohol suspension to DBD plasma treatment, resulting in a reduction of particle size and an increase in solubility compared to the untreated solution.

The impact of various sterilization methods on the turbidity of salmon MP was significantly, as illustrated in Fig. 1A. The turbidity of MP in untreated salmon was 0.86, whereas that of PAW (0.89), SAEW (1.01) and PASW (0.77) exhibited different levels. During the treatment of PAW and SAEW, hydrophobic groups were exposed and molecular interactions increased, leading to the aggregation of monomeric proteins into insoluble proteins, resulting in increased turbidity. Compared to the control, the turbidity of MP treated with PASW was reduced notably ($P < 0.05$), which can be attributed to a decrease in particle size

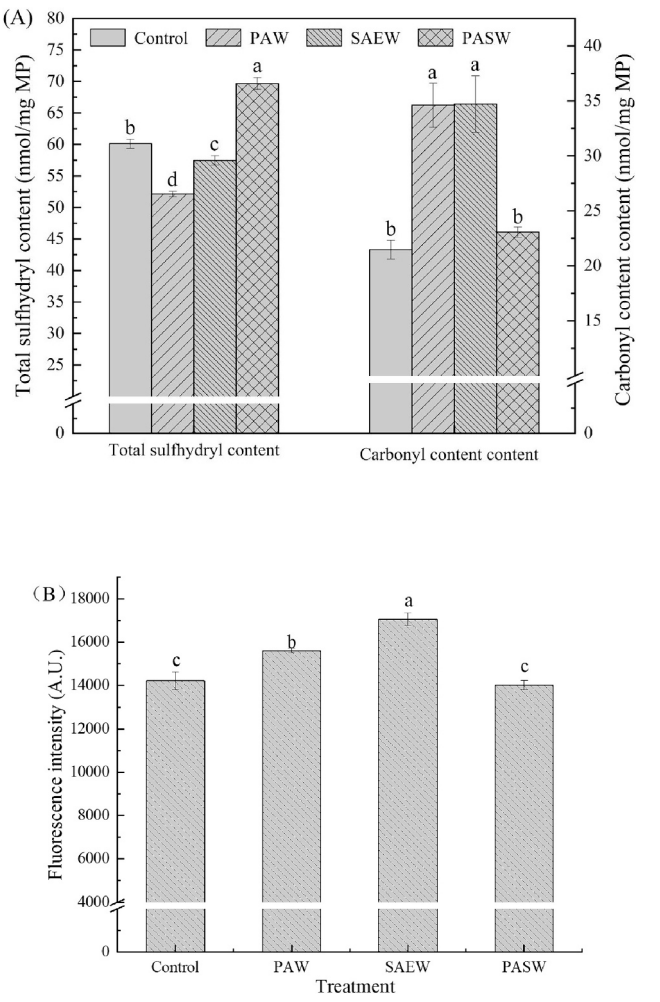

Fig. 2. Effects of different sterilizing methods on total sulfhydryl groups, carbonyl groups content (A) and dityrosine content (B) of myofibrillar protein. Control, fresh salmon; PAW, plasma activation of water; SAEW, slightly acidic electrolytic water; PASW, low-temperature plasma assisted slightly acidic electrolytic water. Different letters (a-d) show statistically significant difference ($P < 0.05$).

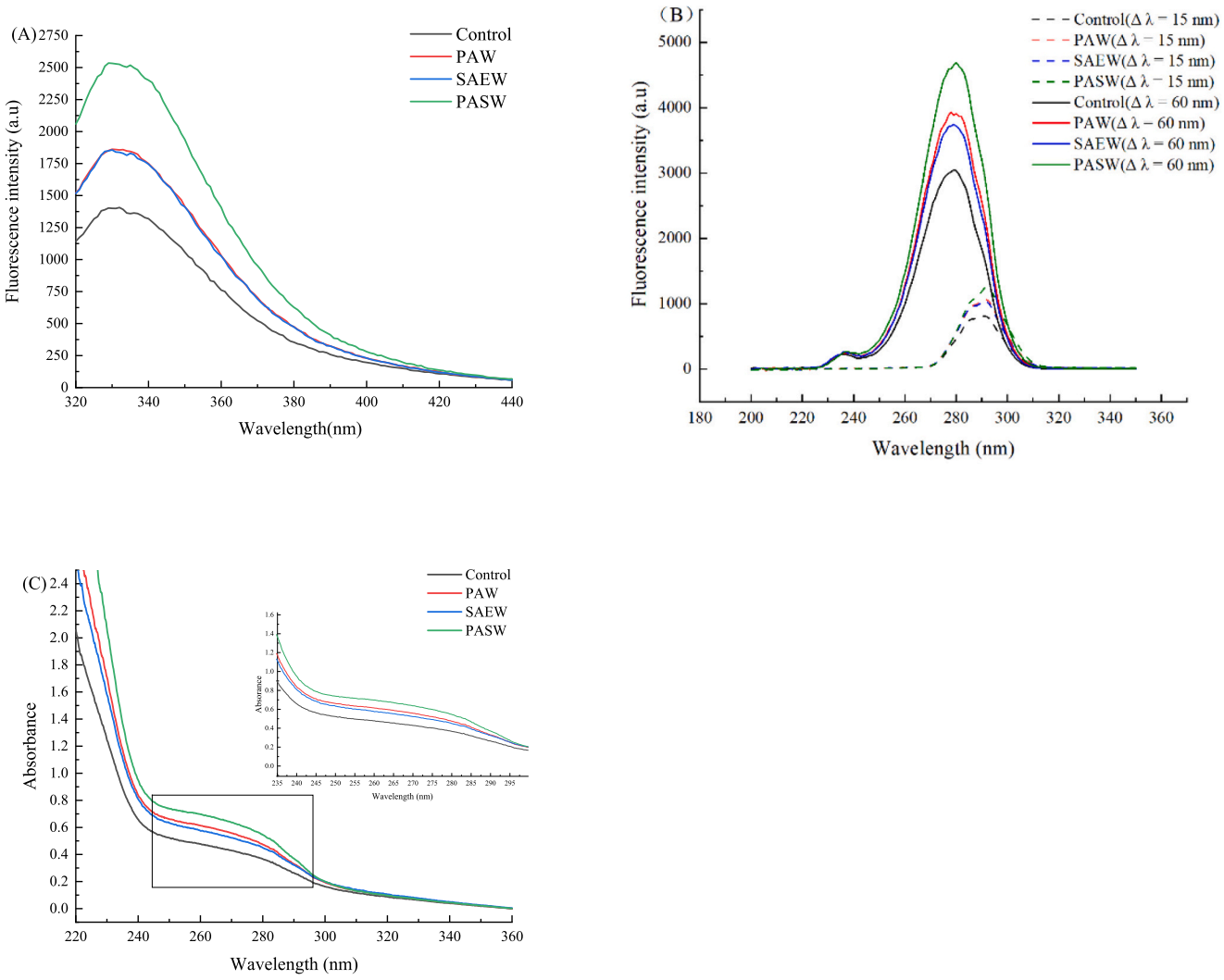

Fig. 3. Effects of different sterilizing methods on intrinsic fluorescence spectra (A); synchronous fluorescence spectra (B) and Ultraviolet and visible spectrum (C) of myofibrillar protein. Control, fresh salmon; PAW, plasma activation of water; SAEW, slightly acidic electrolytic water; PASW, low-temperature plasma assisted slightly acidic electrolytic water. Different letters (a-d) show statistically significant difference ($P < 0.05$).

distribution and an increase in specific surface area (Amiri et al., 2021).

3.1.2. *Surface hydrophobicity*

Surface hydrophobicity reflects the degree of exposure of hydrophobic groups on protein molecules. As the surface exposure of hydrophobic groups increases, protein denaturation becomes more severe (Ekezie et al., 2019). Bromophenol blue can bind to the hydrophobic region of a protein, and thus the amount of bromophenol blue binding can serve as an indicator for the surface hydrophobicity of MP. Furthermore, there exists a positive correlation between these two factors (Jia, Wang, Shao, Liu, & Kong, 2017). The untreated fresh salmon MP had a surface hydrophobicity of 37.66 μg, whereas the bactericidal treatments significantly altered the surface hydrophobicity of MP. Specifically, treatment with PAW (41.56 μg) and SAEW (39.51 μg) resulted in a significant increase in the surface hydrophobicity of salmon MP (Fig. 1B). This effect is likely due to the active substances in SAEW and PAW inducing hydrogen bonding, electrostatic interactions, and hydration between protein molecules, leading to their unfolding and exposure of previously buried hydrophobic groups to a polar environment (Sharma & Singh, 2020). Hence, the hydrophobicity of the protein surface is enhanced. In contrast, the surface hydrophobicity of salmon MP treated with PASW (35.30 μg) was significantly reduced, potentially attributed to the alteration in electrostatic interactions of MP induced by the active substance present in PASW. Further investigation is required to elucidate the specific underlying mechanisms.

3.2. *Protein oxidation*

3.2.1. *Total sulfhydryl and carbonyl*

Sulfhydryl groups play a crucial role in modulating protein activity, and their oxidation to form disulfide bonds results in a reduction of sulfhydryl content (He et al., 2018). The total sulfhydryl content exhibited significant differences among all treatment groups (Fig. 2A), with PASW showing the highest level (69.67 nmol/mg MP), followed by control, SAEW and PAW in descending order. The decrease in the content of MP total sulfhydryl group treated by PAW and SAEW may be attributed to alterations in intermolecular forces between protein molecules caused by active substances present in the sterilization solution, leading to protein aggregation and accumulation of significant amounts of sulfhydryl groups on the protein surface (Luo et al., 2022). PASW contains a plethora of active substances, including ions, electrons, and free radicals. These highly reactive agents can modify proteins by breaking disulfide bonds and forming new sulfhydryl groups, meanwhile, the presence of ROS and RNS in PASW can induce oxidative cross-linking between free sulfhydryl groups in proteins, resulting in the formation of novel disulfide bonds (Li et al., 2017). In PASW-treated

salmon fillets, the disulfide bond and C—S bond in protein structure have the lowest cleavage energy. These bonds are susceptible to decomposition in plasma, resulting in a significantly lower formation rate of disulfide bonds compared to their breaking rate (Sharafodin & Soltanizadeh, 2022). Consequently, the overall sulfhydryl content remains relatively high. This indicates that PASW has the potential to inhibit MP oxidation.

During oxidation, peroxyl radicals can readily modify peptide bonds or amino acid side chains, such as lysine. This results in a reduction of sulfhydryl content and an increase in carbonyl content within the protein (Zhang et al., 2021). Consequently, this leads to alterations in the spatial conformation of the protein which ultimately affects its structural and functional properties. The untreated salmon fillets had a carbonyl content of 21.48 nmol/mg, while the highest carbonyl content was observed in salmon fillets treated with SAEW (34.71 nmol/mg). Salmon fillets treated with PAW and PASW had carbonyl contents of 34.61 nmol/mg and 23.06 nmol/mg, respectively (Fig. 2A). The possibility exists that SAEW may oxidize and attack protein, resulting in the formation of novel carbon-centered free radicals. This process can initiate chain reactions of protein free radicals and generate a significant number of carbonyl groups (Sun, Zhao, Yang, Zhao, & Cui, 2011). After the activation of SAEW through low temperature plasma, there may be a change in the types of active substances present in PASW solution. On the other hand, this might be related to the formation of chemical bonds between protein strands and the insoluble aggregates produced due to the reactions/interactions of carbonyl groups. Also, the appearance of protein aggregates decreases the number of amino acid residues on the surface. Therefore, the probability of protein functional groups' exposure to active plasma species diminishes, which directly influences the rate of carbonyl formation (Sharafodin & Soltanizadeh, 2022), thereby weakening PASW oxidation effect on MP carbonyl group.

3.2.2. Dityrosine content

The active species produced during low temperature plasma activation interact with proteins, and the concentration of these species plays a pivotal role in inducing conformational changes to the protein (Sharma & Singh, 2020). The content of dityrosine was significantly elevated in the PAW and SAEW treatment groups compared to the control group (Fig. 2B). However, there was no significant difference between the control group and PASW treatment ($P > 0.05$). The findings suggest that the active substances in PASW may not be sufficient to induce significant oxidation of MP, necessitating further investigation into the specific mechanism.

3.3. MP conformation analysis

3.3.1. Intrinsic fluorescence spectrum

Fluorescence bursts, which were influenced by the polarity of the protein's environment and the interaction between aromatic amino acids such as tyrosine and tryptophan, can serve as a means to determine changes in proteins' tertiary structures (Zhang et al., 2021). At 295 nm, the interference from tyrosine residues can be eliminated, leaving only tryptophan residues to be excited (Heremans & Heremans, 1989). Therefore, changes in the microenvironment of tryptophan residues and tertiary structure of the protein can be reflected by alterations in endogenous fluorescence spectrum intensity (Sun et al., 2011). As depicted in Fig. 3A, MP treated with various sterilization methods exhibited alterations when compared to untreated MP. The peak shapes of PAW and SAEW were essentially identical, with no differences in fluorescence intensity. However, the fluorescence intensity of PASW was the strongest. The tryptophan side chain group was gradually exposed to the solvent from the internal hydrophobic region, increasing the polarity of its microenvironment and enhancement of fluorescence intensity. Studies have demonstrated that the λ_{max} value is indicative of the microenvironment surrounding the tryptophan residue, with a λmax <330 nm suggesting that the residue is situated in a non-polar

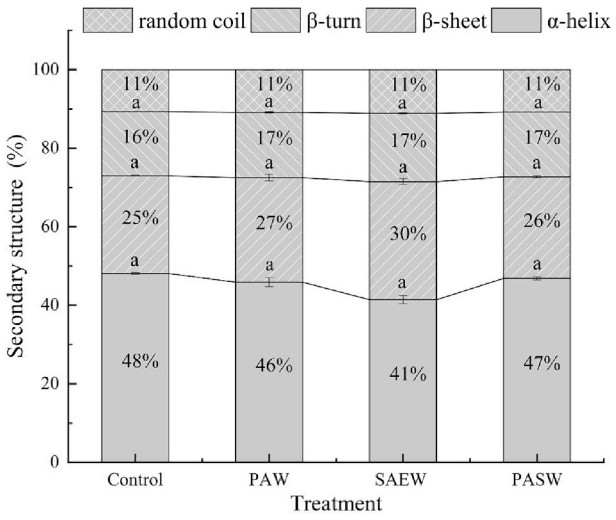

Fig. 4. Effect of different sterilization methods on secondary structure of myofibrillar protein. Control, fresh salmon; PAW, plasma activation of water; SAEW, slightly acidic electrolytic water; PASW, low-temperature plasma assisted slightly acidic electrolytic water. The lowercase letter (a) shows the difference is not statistically significant ($P > 0.05$).

environment within the protein molecule, and a λmax >330 nm indicating that it is located in a polar environment outside of the protein molecule (Zhou et al., 2014). The λmax values of MP in this experiment were predominantly centered around 332 nm, suggesting that the tryptophan residues had likely been translocated to the exterior of the protein molecule and exposed to a polar environment. The alteration of the tryptophan microenvironment indicates that different sterilization methods have an impact on the tertiary structure of MP. The modification of protein structure by CP varies depending on the type of gas used and the exposure and generator settings of the sample. Ekezie et al. (2019) utilized an atmospheric pressure plasma jet to directly treat the MP of king prawn (*Litopenaeus vannamei*), resulting in a reduction of peak UV spectra in proteins compared to untreated samples.

3.3.2. Synchronous fluorescence spectrum

Synchronous fluorescence spectra offer insights into the polarity of the fluorophore's microenvironment, while the maximum fluorescence peak value indicates changes in protein conformation (Liu, Lu, Han, Chen, & Kong, 2015). The synchrotron fluorescence spectra of salmon MP under different sterilization methods are presented in Fig. 3B, with (a) indicating tyrosine residues (Δ λ = 15 nm) and (b) representing tryptophan residues (Δ λ = 60 nm). The fluorescence emission peaks of tyrosine and tryptophan residues in the MP treated with PAW and SAEW were slightly red-shifted, indicating a more polar and less hydrophobic microenvironment surrounding these two amino acid residues (Shen et al., 2019). Compared to tyrosine residues, tryptophan residues exhibit higher fluorescence emission intensity. In other words, the endogenous fluorescence of MP primarily originates from tryptophan residues.

3.3.3. UV absorption spectrum

Typically, the UV absorption spectra of natural proteins were mainly dominated by aromatic amino acid residues, particularly tyrosine and tryptophan residues (Ekezie et al., 2019). Therefore, UV spectroscopy was commonly used to evaluate changes in the microenvironment of aromatic amino acid side chains and chromophores, which in turn reflect changes in the tertiary structure of proteins. As can be seen from Fig. 3C, the characteristic absorption peak of PASW were higher, followed by PAW and SAEW. The increase in the UV absorption intensity of MP may be due to the structural unfolding of the protein in the presence of active substances, and the transfer of chromogenic groups such as tryptophan and tyrosine from a non-polar environment to a polar one,

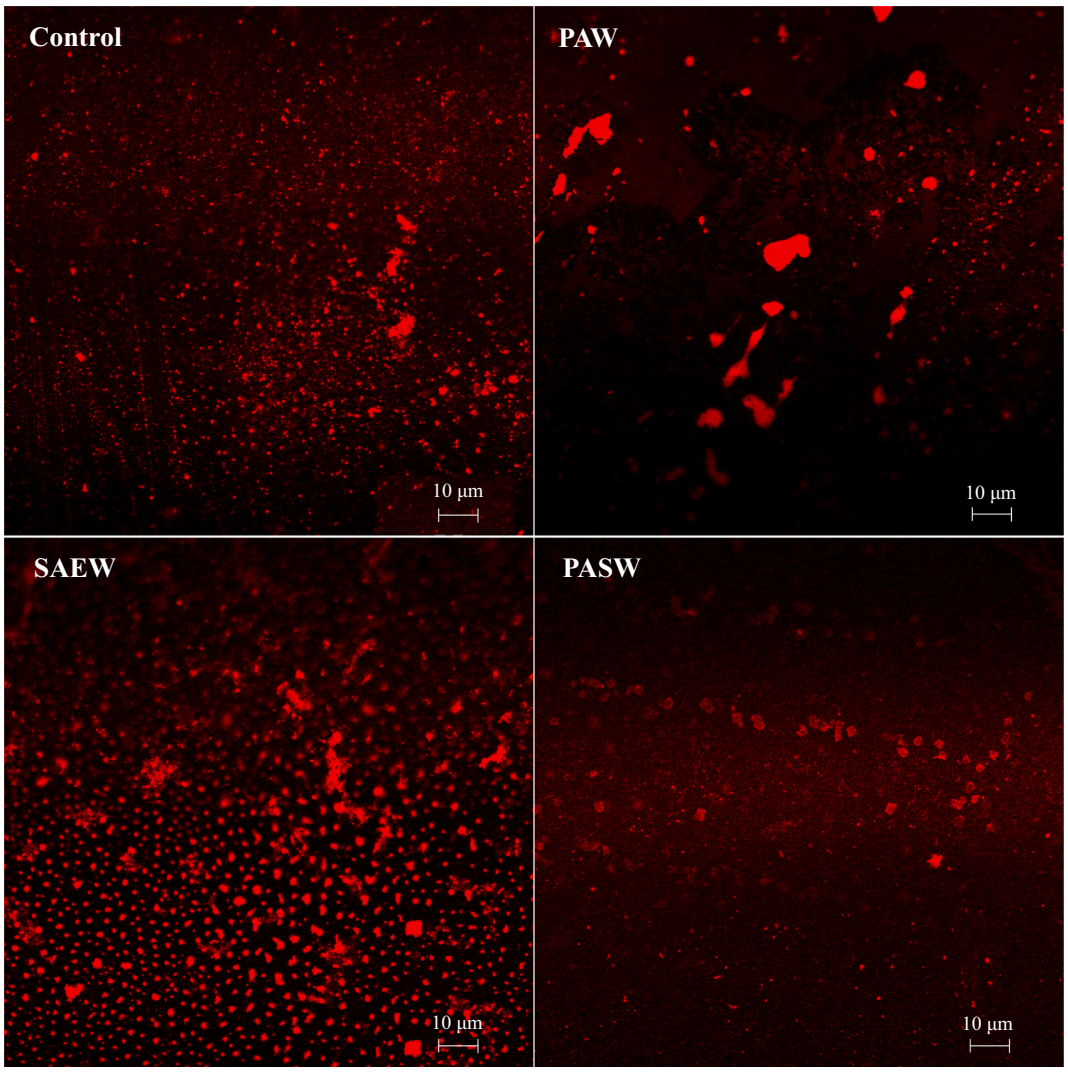

Fig. 5. Confocal laser image of myofibrillar protein under different sterilization methods. Control, fresh salmon; PAW, plasma activation of water; SAEW, slightly acidic electrolytic water; PASW, low-temperature plasma assisted slightly acidic electrolytic water. Different letters (a-d) show statistically significant difference ($P < 0.05$).

which ultimately enhances the protein's UV absorption intensity.

3.3.4. *Raman spectrum*

As depicted in Fig. 4, the predominant secondary structures of salmon MP were α-helix and β-fold, accounting for approximately 48% and 25%, respectively. In comparison to the control group, treatment with PASW resulted in a slight reduction of α-helix content and a minor increase in β-fold content. The active compounds in salmon MP treated with PAW and SAEW can induce conformational changes in protein secondary structures, specifically transitioning from α-helix to β-folding. The observed phenomenon may be attributed to protein denaturation, which disrupts the interaction between certain non-covalent bonds and consequently leads to a structural alteration in the protein. The previous study discovered that CP had a negligible impact on the secondary structure of maize alcohol proteins (Dong et al., 2017), whereas Misra et al. (2015) investigated the influence of atmospheric pressure plasma jet (APPJ) on wheat flour structure and observed an increase in α-helix and β-turn content, accompanied by a decrease in β-fold content. Sharifian, Soltanizadeh, and Abbaszadeh (2019) investigated the direct treatment of beef myofibrillar protein with DBD plasma. The results demonstrated that after 10 min of MP treated by DBD, the α-helix content decreased and the protein structure unfolded, while significant increases in β-folding and β-turn angle were observed after 20 min of treatment. The increase in β-folding and decrease in α-helix content are typically attributed to protein denaturation and unfolding (Li et al., 2019). Furthermore, a negative linear correlation was observed between surface hydrophobicity and α-helix content. Thus, disruption of the α-helix structure is accompanied by an increase in surface hydrophobicity.

3.4. *Microstructural analysis*

LSCM was capable of visualizing the morphological changes in MP, which bound to Nile blue fluorescent marker and exhibited a red appearance under an excitation wavelength of 633 nm. As depicted in Fig. 5, the untreated MP particles exhibited satisfactory dispersion and relatively uniform distribution. After PAW treatment, MP exhibited aggregation into large particles characterized by significant size disparities and uneven distribution. Those treated with SAEW displayed substantial aggregation while maintaining a uniform distribution among the particles. Conversely, the MP of PASW treatment exhibited a slight degree of aggregation while still maintaining a uniform distribution among the particles. Plasma is composed of positive and negative ions, free radicals, UV photons, electrons, as well as excited or unexcited molecules and atoms, which energetic species have the ability to cleave covalent bonds and initiate diverse chemical reactions (Kim, Lee, & Min,

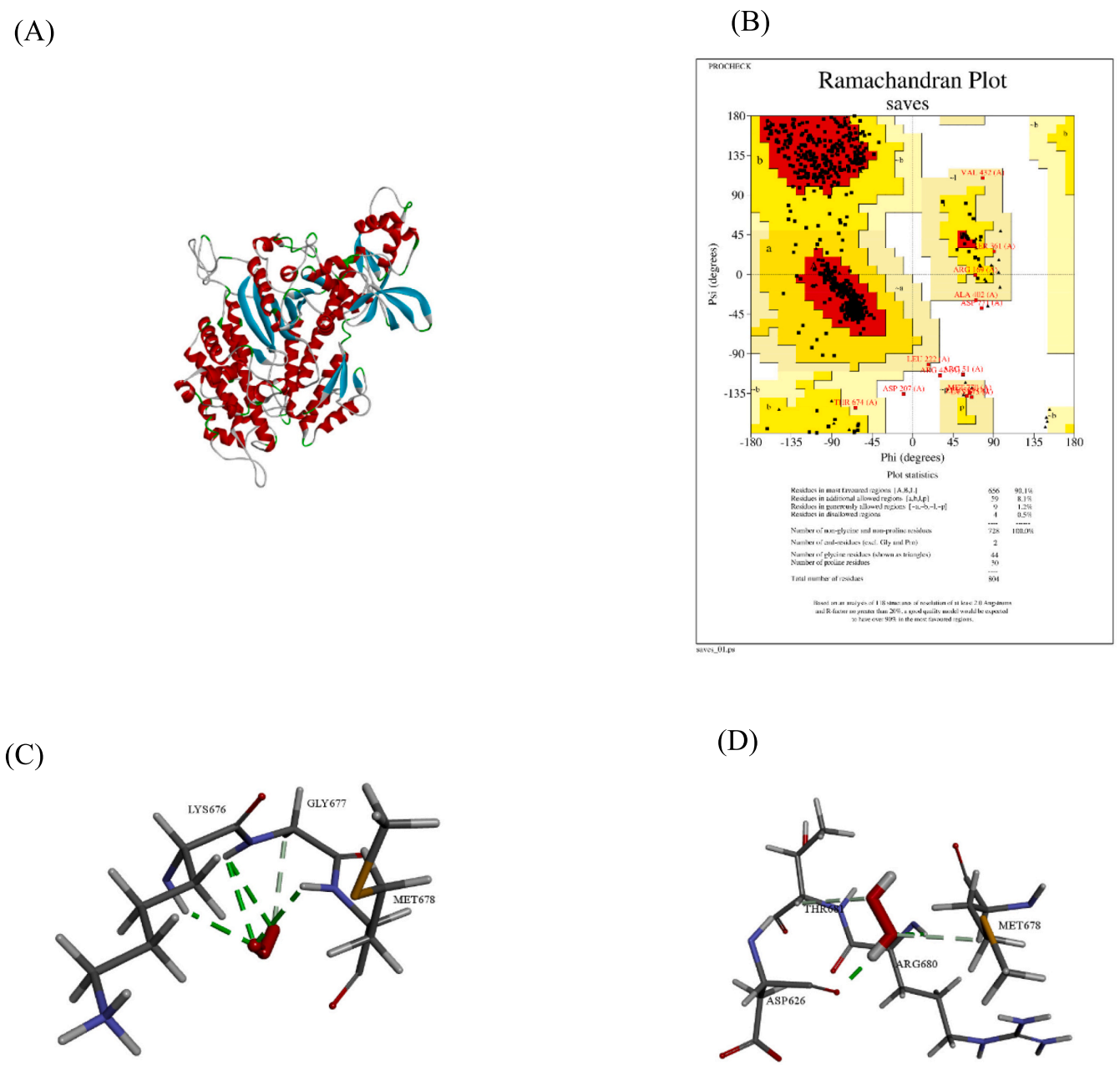

Fig. 6. Salmon myosin modeling structure (A), pull-diagram analysis (B), and three-dimensional diagram of interaction between O_3 (C), H_2O_2 (D) with myosin. Control, fresh salmon; PAW, plasma activation of water; SAEW, slightly acidic electrolytic water; PASW, low-temperature plasma assisted slightly acidic electrolytic water. Different letters (a-d) show statistically significant difference ($P < 0.05$).

2014). The low degree of MP aggregation observed after PASW treatment may be attributed to the disruption of intermolecular forces that maintain aggregate conformation by CP treatment. Furthermore, the reduction in surface hydrophobicity also impacted the degree of aggregation (Song, Oh, Roh, Kim, & Min, 2016).

3.5. Molecular docking analysis

ROS refers to both free radicals and non-free radicals generated from oxygen sources, with H_2O_2 and O_3 being the most significant molecular species. In the present study, we conducted a molecular docking analysis to identify receptor binding sites on myosin for H_2O_2 and O_3 regulatory targets. The three-dimensional architecture of salmon myosin, as constructed in this experiment, is depicted in Fig. 6a. As can be seen from Fig. 6b, the fully allowed region contained 90.1% of the amino acids, while the allowed region accounted for 8.1%. These results suggest that the model derived from homology modeling of salmon myosin is applicable. The binding sites of the O_3 and myosin were Lys676, Gly677 and Met678, and the binding force of O_3 to the myosin was hydrogen bonding (Fig. 6c). Meanwhile, the binding sites of the H_2O_2 and myosin were Thr681, Asp626, Arg680 and Met678, and the binding force of O_3 to the myosin was hydrogen bonding (Fig. 6d). Met678 is a crucial binding site for ligands (H_2O_2 and O_3) to interact with the receptor salmon myosin. The docking results indicate that H_2O_2 plays a crucial role in the myosin structure, as its docking energy (−11.418 kcal/mol) is significantly lower than that of O_3 (−3.775 kcal/mol). Rathore and Nema (2021) have also confirmed this finding, noting that the H_2O_2 concentration in PAW changes by only 1.54% after two weeks of storage at 4 °C. However, dissolved O_3 concentrations decreased significantly during the same period.

4. Conclusion

The PASW-treated MP exhibited reduced aggregation and enhanced stability compared to other sterilization methods. PASW treatment can effectively mitigate damage to the secondary and tertiary structures of MP. Molecular docking analysis reveals that Met678 serves as the crucial binding site for ligands (H_2O_2 and O_3) to interact with the myosin receptor. Notably, H_2O_2 exhibits a more pronounced effect on salmon myosin compared to O_3. In conclusion, compared with other sterilization methods, PASW treatment better preserves the physicochemical properties of MP and mitigates changes in protein structure, making it a more promising method for sterilizing aquatic products. The bactericidal efficacy of PASW is influenced by various factors, including the parameters of low temperature plasma equipment and the type of sample, which require further investigation prior to practical implementation in the food industry.

CRediT authorship contribution statement

Guizhi Tan: Writing – original draft, Formal analysis, Data curation. **Yue Ning:** Writing – original draft, Data curation. **Chaonan Sun:** Investigation, Data curation. **Ying Bu:** Visualization, Supervision, Project administration, Investigation. **Xiaomin Zhang:** Writing – review & editing. **Wenhui Zhu:** Writing – review & editing, Validation, Methodology, Data curation. **Jianrong Li:** Supervision, Project administration, Conceptualization. **Xuepeng Li:** Writing – review & editing, Supervision, Project administration, Methodology, Conceptualization.

Declaration of competing interest

The authors have declared that no competing interest to declare. This manuscript has not been published and is not under consideration for publication in any other journal.

Data availability

The data that has been used is confidential.

Acknowledgement

This study was supported by the National Key Research and Development Program of China (2019YFD0901702) and the Open Fund of Institute of Ocean Research, Bohai University (BDHYYJY2023004).

References

Amiri, A., Sharifian, P., Morakabati, N., Mousakhani-Ganjeh, A., Mirtaheri, M., Nilghaz, A., Guo, Y.-G., & Pratap-Singh, A. (2021). Modification of functional, rheological and structural characteristics of myofibrillar proteins by high-intensity ultrasonic and papain treatment. *Innovative Food Science & Emerging Technologies, 72*, Article 102748. https://doi.org/10.1016/j.ifset.2021.102748

Cao, W., Zhu, Z. W., Shi, Z. X., Wang, C. Y., & Li, B. M. (2009). Efficiency of slightly acidic electrolyzed water for inactivation of Salmonella enteritidis and its contaminated shell eggs. *International Journal of Food Microbiology, 130*(2), 88–93. https://doi.org/10.1016/j.ijfoodmicro.2008.12.021

Cheng, J., Zhu, M., & Liu, X. (2020). Insight into the conformational and functional properties of myofibrillar protein modified by mulberry polyphenols. *Food Chemistry, 308*, Article 125592. https://doi.org/10.1016/j.foodchem.2019.125592

Cichoski, A. J., Flores, D. R. M., De Menezes, C. R., Jacob-Lopes, E., Zepka, L. Q., Wagner, R., … Campagnol, P. C. B. (2019). Ultrasound and slightly acid electrolyzed water application: An efficient combination to reduce the bacterial counts of chicken breast during pre-chilling. *International Journal of Food Microbiology, 301*, 27–33. https://doi.org/10.1016/j.ijfoodmicro.2019.05.004

Davies, K. J., Delsignore, M. E., & Lin, S. W. (1987). Protein damage and degradation by oxygen radicals. II. Modification of amino acids. *Journal of Biological Chemistry, 262*(20), 9902–9907. https://doi.org/10.1016/S0021-9258(18)48019-2

Dong, S., Wang, J. M., Cheng, L. M., Lu, Y. L., Li, S. H., & Chen, Y. (2017). Behavior of zein in aqueous ethanol under atmospheric pressure cold plasma treatment. *Journal of Agricultural and Food Chemistry, 65*(34), 7352–7360. https://doi.org/10.1021/acs.jafc.7b02205

Ekezie, F. C., Cheng, J. H., & Sun, D. W. (2019). Effects of atmospheric pressure plasma jet on the conformation and physicochemical properties of myofibrillar proteins from king prawn (*Litopenaeus vannamei*). *Food Chemistry, 276*, 147–156. https://doi.org/10.1016/j.foodchem.2018.09.113

Feizollahi, E., Misra, N. N., & Roopesh, M. S. (2021). Factors influencing the antimicrobial efficacy of Dielectric Barrier Discharge (DBD) Atmospheric Cold Plasma (ACP) in food processing applications. *Critical Reviews in Food Science and Nutrition, 61*(4), 666–689. https://doi.org/10.1080/10408398.2020.1743967

He, Y., Huang, H., Li, L., Yang, X., Hao, S., Chen, S., & Deng, J. (2018). The effects of modified atmosphere packaging and enzyme inhibitors on protein oxidation of tilapia muscle during iced storage. *LWT- Food Science and Technology, 87*, 186–193. https://doi.org/10.1016/j.lwt.2017.08.046

Heremans, L., & Heremans, K. (1989). Raman spectroscopic study of the changes in secondary structure of chymotrypsin: Effect of pH and pressure on the salt bridge. *Biochimica et Biophysica Acta (BBA) - Protein Structure and Molecular Enzymology, 999*(2), 192–197. https://doi.org/10.1016/0167-4838(89)90217-3

Jia, N., Wang, L., Shao, J., Liu, D., & Kong, B. (2017). Changes in the structural and gel properties of pork myofibrillar protein induced by catechin modification. *Meat Science, 127*, 45–50. https://doi.org/10.1016/j.meatsci.2017.01.004

Kim, J. E., Lee, D. U., & Min, S. C. (2014). Microbial decontamination of red pepper powder by cold plasma. *Food Microbiology, 38*, 128–136. https://doi.org/10.1016/j.fm.2013.08.019

Li, F., Wang, B., Liu, Q., Chen, Q., Zhang, H., Xia, X., & Kong, B. (2019). Changes in myofibrillar protein gel quality of porcine longissimus muscle induced by its structural modification under different thawing methods. *Meat Science, 147*, 108–115. https://doi.org/10.1016/j.meatsci.2018.09.003

Li, J., Xiang, Q., Liu, X., Ding, T., Zhang, X., Zhai, Y., & Bai, Y. (2017). Inactivation of soybean trypsin inhibitor by dielectric-barrier discharge (DBD) plasma. *Food Chemistry, 232*, 515–522. https://doi.org/10.1016/j.foodchem.2017.03.167

Li, N., Yu, J. J., Jin, N., Chen, Y., Li, S. H., & Chen, Y. (2020). Modification of the physicochemical and structural characteristics of zein suspension by dielectric barrier discharge cold plasma treatment. *Journal of Food Science, 85*(8), 2452–2460. https://doi.org/10.1111/1750-3841.15350

Li, X., Sun, T., Zhang, X. R., Hou, C., Shen, Q., Wang, D., & Ni, G. H. (2023). Low temperature plasma suppresses proliferation, invasion, migration and survival of SK-BR-3 breast cancer cells. *Molecular Biology Reports, 50*(3), 2025–2031. https://doi.org/10.1007/s11033-022-08026-4

Liu, Q., Lu, Y., Han, J., Chen, Q., & Kong, B. (2015). Structure-modification by moderate oxidation in hydroxyl radical-generating systems promote the emulsifying properties of soy protein isolate. *Food Structure, 6*, 21–28. https://doi.org/10.1016/j.foostr.2015.10.001

Liu, Y., Bu, Y., Zhu, W., Li, J., & Li, X. (2023). Effects of divalent mercury on myosin structure of large yellow croaker and its binding mechanism: Multi-spectroscopies and molecular docking. *Food Chemistry, 418*, Article 135972. https://doi.org/10.1016/j.foodchem.2023.135972

Luo, J., Xu, W., Liu, Q., Zou, Y., Wang, D., & Zhang, J. (2022). Dielectric barrier discharge cold plasma treatment of pork loin: Effects on muscle physicochemical properties and emulsifying properties of pork myofibrillar protein. *LWT- Food Science and Technology, 162*, Article 113484. https://doi.org/10.1016/j.lwt.2022.113484

Ma, M., Zhang, Y., Lv, Y., & Sun, F. (2020). The key reactive species in the bactericidal process of plasma activated water. *Journal of Physics D: Applied Physics, 53*(18), Article 185207. https://doi.org/10.1088/1361-6463/ab703a

Misra, N. N., Kaur, S., Tiwari, B. K., Kaur, A., Singh, N., & Cullen, P. J. (2015). Atmospheric pressure cold plasma (ACP) treatment of wheat flour. *Food Hydrocolloids, 44*, 115–121. https://doi.org/10.1016/j.foodhyd.2014.08.019

Nyaisaba, B. M., Miao, W., Hatab, S., Siloam, A., Chen, M., & Deng, S. (2019). Effects of cold atmospheric plasma on squid proteases and gel properties of protein concentrate from squid (*Argentinus ilex*) mantle. *Food Chemistry, 291*, 68–76. https://doi.org/10.1016/j.foodchem.2019.04.012

Olatunde, O. O., & Benjakul, S. (2018). Nonthermal processes for shelf-life extension of seafoods: A revisit. *Comprehensive Reviews in Food Science and Food Safety, 17*(4), 892–904. https://doi.org/10.1111/1541-4337.12354

Pan, T., Guo, H., Li, Y., Song, J., & Ren, F. (2017). The effects of calcium chloride on the gel properties of porcine myosin–κ-carrageenan mixtures. *Food Hydrocolloids, 63*, 467–477. https://doi.org/10.1016/j.foodhyd.2016.09.026

Pankaj, S. K., Wan, Z., & Keener, K. M. (2018). Effects of cold plasma on food quality: A review. *Foods, 7*(1), 4. https://doi.org/10.3390/foods7010004

Perez-Andres, J. M., Charoux, C. M. G., Cullen, P. J., & Tiwari, B. K. (2018). Chemical modifications of lipids and proteins by nonthermal food processing technologies. *Journal of Agricultural and Food Chemistry, 66*(20), 5041–5054. https://doi.org/10.1021/acs.jafc.7b06055

Qian, J., Wang, C., Zhuang, H., Nasiru, M. M., Zhang, J., & Yan, W. (2021). Evaluation of meat-quality and myofibrillar protein of chicken drumsticks treated with plasma-activated lactic acid as a novel sanitizer. *LWT- Food Science and Technology, 138*, Article 110642. https://doi.org/10.1016/j.lwt.2020.110642

Rathore, V., & Nema, S. K. (2021). Optimization of process parameters to generate plasma activated water and study of physicochemical properties of plasma activated solutions at optimum condition. *Journal of Applied Physics, 129*, Article 084901. https://doi.org/10.1063/5.0033848

Sharafodin, H., & Soltanizadeh, N. (2022). Potential application of DBD plasma technique for modifying structural and physicochemical properties of soy protein isolate. *Food Hydrocolloids, 122*, Article 107077. https://doi.org/10.1016/j.foodhyd.2021.107077

Sharifian, A., Soltanizadeh, N., & Abbaszadeh, R. (2019). Effects of dielectric barrier discharge plasma on the physicochemical and functional properties of myofibrillar proteins. *Innovative Food Science & Emerging Technologies, 54*, 1–8. https://doi.org/10.1016/j.ifset.2019.03.006

Sharma, S., & Singh, R. K. (2020). Cold plasma treatment of dairy proteins in relation to functionality enhancement. *Trends in Food Science & Technology, 102*, 30–36. https://doi.org/10.1016/j.tifs.2020.05.013

Shen, H., Zhao, M., & Sun, W. (2019). Effect of pH on the interaction of porcine myofibrillar proteins with pyrazine compounds. *Food Chemistry, 287*, 93–99. https://doi.org/10.1016/j.foodchem.2019.02.060

Song, A. Y., Oh, Y. A., Roh, S. H., Kim, J. H., & Min, S. C. (2016). Cold oxygen plasma treatments for the improvement of the physicochemical and biodegradable properties of polylactic acid films for food packaging. *Journal of Food Science, 81*(1), 86–96. https://doi.org/10.1111/1750-3841.13172

Sun, C., Dai, L., Liu, F., & Gao, Y. (2016). Simultaneous treatment of heat and high pressure homogenization of zein in ethanol–water solution: Physical, structural, thermal and morphological characteristics. *Innovative Food Science & Emerging Technologies, 34*, 161–170. https://doi.org/10.1016/j.ifset.2016.01.016

Sun, W., Zhao, M., Yang, B., Zhao, H., & Cui, C. (2011). Oxidation of sarcoplasmic proteins during processing of Cantonese sausage in relation to their aggregation behaviour and in vitro digestibility. *Meat Science, 88*(3), 462–467. https://doi.org/10.1016/j.meatsci.2011.01.027

Zhang, Q., Cheng, Z., Zhang, J., Nasiru, M. M., Wang, Y., & Fu, L. (2021). Atmospheric cold plasma treatment of soybean protein isolate: Insights into the structural, physicochemical, and allergenic characteristics. *Journal of Food Science, 86*(1), 68–77. https://doi.org/10.1111/1750-3841.15556

Zhao, W., & Yang, R. (2012). Pulsed electric field induced aggregation of food proteins: Ovalbumin and bovine serum albumin. *Food and Bioprocess Technology, 5*(5), 1706–1714. https://doi.org/10.1007/s11947-010-0464-8

Zhou, A., Lin, L., Liang, Y., Benjakul, S., Shi, X., & Liu, X. (2014). Physicochemical properties of natural actomyosin from threadfin bream (*Nemipterus spp.*) induced by high hydrostatic pressure. *Food Chemistry, 156*, 402–407. https://doi.org/10.1016/j.foodchem.2014.02.013

Zhu, W., Guo, H., Han, M., Shan, C., Bu, Y., Li, J., & Li, X. (2022). Evaluating the effects of nanoparticles combined ultrasonic-microwave thawing on water holding capacity, oxidation, and protein conformation in jumbo squid (*Dosidicus gigas*) mantles. *Food Chemistry, 402*, Article 134250. https://doi.org/10.1016/j.foodchem.2022.134250

Zhu, W., Tan, G., Han, M., Bu, Y., Li, X., & Li, J. (2023). Evaluating the effects of plasma-activated slightly acidic electrolyzed water on bacterial inactivation and quality attributes of Atlantic salmon fillets. *Innovative Food Science & Emerging Technologies, 84*, Article 103286. https://doi.org/10.1016/j.ifset.2023.103286